A&A 420, 383–388 (2004)
DOI: 10.1051/0004-6361:20034507

Astronomy & Astrophysics

A study of Trans-Neptunian object 55636 (2002 TX_{300})

J. L. Ortiz[1], A. Sota[1], R. Moreno[2], E. Lellouch[3], N. Biver[3], A. Doressoundiram[3], P. Rousselot[4], P. J. Gutiérrez[1,5], I. Márquez[1], R. M. González Delgado[1], and V. Casanova[1]

[1] Instituto de Astrofísica de Andalucía, CSIC, Apt 3004, 18080 Granada, Spain
[2] I.R.A.M., 300 rue de la Piscine, 38406 St-Martin d'Hères Cedex, France
[3] Observatoire de Paris, 5 place J. Jansen, 92195 Meudon, France
[4] Observatoire de Besançon, BP 1615, 25010 Besançon Cedex, France
[5] Laboratoire d'Astrophysique de Marseille, Traverse du Siphon, BP 8, 13376 Marseille Cedex 12, France

Received 13 October 2003 / Accepted 3 March 2004

Abstract. We report on physical properties of the bright Trans-Neptunian Object 2003 TX_{300} based on a large set of observations taken in different wavelength ranges. Broad band CCD observations aimed at studying the short-term rotational variability show a low amplitude periodic signal of 7.89 ± 0.03 h. We cannot yet determine whether the lightcurve is single-peaked (i.e. the rotation period would be 7.89 h) or double-peaked (i.e. the actual spin period would be 15.78 h). From a sinusoidal fit, the peak to peak amplitude of the brightness changes is 0.09 ± 0.08 mag. If the brightness changes are due to irregular shape, this amplitude implies a minimum axial ratio of 1.09. *BVRI* photometry indicates similar colors as other large Kuiper Belt members, with $B - V = 0.64 \pm 0.04$, $V - R = 0.40 \pm 0.07$, and $R - I = 0.22 \pm 0.05$. Thermal observations at 250 GHz (1.2 mm) result in no confident detection of the body, with a measured flux of 0.22 ± 0.51 mJy. Combining all the data and using the same thermophysical model as in Lellouch et al. (2002) we find (at a 3-σ confidence level) a lower limit for the geometric albedo ($p_v > 0.06$) and an upper limit for the size of this object ($D < 1110$ km). A more relaxed 2-σ confidence level implies a diameter $D < 907$ km and an albedo $p_v > 0.08$, which is significantly higher than the typical 0.04 cometary value and also higher than that of Varuna.

Key words. minor planets, asteroids – Kuiper Belt

1. Introduction

Large Trans-Neptunian Objects (TNOs) are important bodies because they are the only Kuiper Belt objects for which a significant number of properties can be derived. Their brightness is just sufficient for the largest telescopes in the world to observe them in spectroscopy mode, which gives us important hints on composition and surface properties. Other observing techniques can be applied; in particular, their thermal emission can be measured in order to derive albedos and sizes. Except for the specific case of binary objects, physical information on TNOs is very limited. Broad band *BVRI* photometry aimed at deriving color information is feasible with most of the TNOs, but spectroscopic and other detailed studies are restricted to large TNOs.

Very large TNOs like 50 000 Quaoar, 20 000 Varuna, 28 978 Ixion, 38 628 Huya (2000 EB_{173}), 2002 AW_{197}, etc. have been studied in some detail and important properties have been derived (see e.g. Jewitt & Sheppard 2002; Brown & Trujillo 2004). Perhaps one of the most remarkable findings is the fact that they may be "rubble pile" low-density very porous objects not far from critical rotation (with rotation periods close to the value for which the centrifugal force can break up the body). Their shapes may therefore be considerably distorted (at least in the case of Varuna) as a response to rotation (Jewitt & Sheppard 2002).

In October 2002 a potentially very large new TNO with designation 2002 TX_{300} was discovered, which offered an excellent opportunity to increase our knowledge on the Kuiper Belt. With that goal in mind, we tried to get as much information on 2002 TX_{300} as possible. Coordinated observational campaigns were arranged on 4 different telescopes with the aim of deriving several important properties, including albedo, for which thermal observations in the millimetric range were needed in combination with optical data. The longest observing runs were devoted to determining the period and amplitude of the suspected short-term variability due to rotation. Other runs were scheduled for regular high signal-to-noise *BVRI* photometry. The main results of the coordinated campaign are summarized here.

2. Observations and data reduction

A log of the observations is shown in Table 1.

Send offprint requests to: J. L. Ortiz, e-mail: ortiz@iaa.es

Table 1. Dates and geometric data (range) of the observations. r_h is heliocentric distance, Δ is geocentric distance and α is phase angle.

Telescope	Observing dates (UT)	r_h (AU)	Δ (AU)	α (deg)
CFHT 3.6 m	29, 30 Oct. (2002)	40.74	39.89–39.90	0.73–0.75
NOT 2.5 m	6, 7 Nov. (2002)	40.74	39.96–39.97	0.86–0.88
OSN 1.5 m	28–30 Nov. (2002)	40.75	40.22–40.25	1.18–1.20
OSN 1.5 m	2, 3, 4, 6 Dec. (2002)	40.75	40.28–40.34	1.22–1.26
IRAM 30 m	6,7,12 Dec. (2002)	40.76	40.34–40.42	1.26–1.30
IRAM 30 m	28 Jan. (2003)	40.77	41.20	1.23
IRAM 30 m	3 Feb. (2003)	40.77	41.29	1.17
IRAM 30 m	11, 12 Mar. (2003)	40.78	41.66	0.64–0.63

2.1. Observations of 2002 TX_{300} at Sierra Nevada observatory

The CCD observations focused on short-term variability were carried out with the Instituto de Astrofísica de Andalucía 1.5 m telescope at Sierra Nevada Observatory, in Granada, Spain. The data were obtained on November 28, 29, 30 and on December 2, 3, 4 and 6, 2002.

The typical exposure time was 100 s (short enough to avoid noticeable trailing under the best seeing conditions, but long enough so that the sky background was the dominating noise source). To get a good enough signal to noise ratio, most of the observations were obtained with no filter. The typical seeing during the observations ranged from 1.3 arcsec to 2.2 arcsec, with median around 1.6 arcsec. A fast readout CCD was used so that the overhead was not a significant fraction of the observing nights. The CCD chip format is 1024×1024 pixels and the total field of view is 7 arcmin $\times$ 7 arcmin. The images were bias subtracted in the standard way and flat-fielded using the median of a large set of twilight images. No cosmic ray removal algorithms were used and we simply rejected the few images in which a cosmic ray hit was close to the object. Relative photometry using seven field stars was carried out by means of Daophot routines as implemented in the IDL astronomical library. The synthetic aperture used was typically 8 to 12 pixels in diameter (the smallest possible in order to get the highest signal to noise ratio). These apertures correspond to 3.2 to 4.8 arcsec on the sky. Care was taken not to introduce spurious signals of faint background stars or galaxies in the aperture. In cases where the TNO was close to faint stars or galaxies, the data were rejected. More than 500 images were obtained and a total of 469 images were used.

The typical error bars of the photometry in the individual 100 s integrations were around 0.06 mag. This could be improved considerably by "median averaging" the large amount of relative photometry data points. The approach of averaging is similar to using longer integration times, but has the advantage that no trails are present in the images, cosmic ray hits are fewer and images are also less smeared by errors in the autoguider.

2.2. Observations of 2002 TX_{300} at CFHT

2002 TX_{300} was observed on 29–30 October 2002 and 30–31 October 2002 at the 3.6-m Canada-France-Hawaii telescope. We used the CFH12k panoramic CCD camera, which is a mosaic of 12 2K $\times$ 4K CCD devices, covering a field of 42×28 square arcmin with 0.2 arcsec per pixel. The first night was not photometric with thick cirrus covering most of the sky, and the seeing was 0.8–1.0 arcsec. The second night was photometric. Thus, relative photometry was performed on 2002 TX_{300} the first night and then calibrated on the second night. The 2002 TX_{300} brightness was monitored the first night during almost 6 h through Mould *BVRI* broadband filters.

All the images of 2002 TX_{300} were bias-subtracted using an averaged bias image. They were flat-fielded using the median set of dithered images of the twilight sky. We used the MIDAS package to perform this data processing. Similar processing was performed on the images acquired during the following night and concerning the standard stars and the field containing 2002 TX_{300}.

Since 2002 TX_{300} was observed during a non-photometric night we computed its absolute magnitudes in a two-step process. First we computed the absolute magnitude of five different stars by using the images obtained the following night. These images were obtained with the same filters and the same field of view. It was possible to perform a good photometric reduction for this night by using the IRAF package. Second, we used the same five stars as reference stars for the images containing 2002 TX_{300} and obtained during the non-photometric night. The final absolute magnitudes of 2002 TX_{300} were computed by averaging the five magnitudes computed using the reference stars and their relative difference in magnitude with the target. To obtain a signal-to-noise ratio as good as possible we used a 10-pixel diameter (i.e. about two times the *FWHM*) for the flux measurement of 2002 TX_{300} and of the five reference stars.

2.3. Observations of 2002 TX_{300} at NOT

The observations consisted of 300s integrations in the *R* band, taken on Nov., 6 and 7 with the ALFOSC instrument on the 2.5 m Nordic Optical Telescope at La Palma (Spain). The field of view of the 2048 $\times$ 2048 camera was 6.4 arcmin $\times$ 6.4 arcmin, with a pixel scale of 0.188 arcsec. Four images per night were taken on 2002 TX_{300}, at approximate intervals of one hour. However, one of the images had to be discarded because 2002 TX_{300} was too close to a background object. The images were bias subtracted and flatfielded using a median of twilight sky flats. The photometry was carried out by means of Daophot routines. The photometry was computed relative to 7 field stars. The aperture radius used for the synthetic aperture photometry was 20 pixels (3.8 arcsec). The seeing was of the

order of 2.4 arcsec on the first night and close to 1.2 arcsec on the second night.

2.4. Observations of 2002 TX_{300} at IRAM 30-m

The thermal observations were conducted with the IRAM 30-m radiotelescope in Sierra Nevada (Granada, Spain) on seven dates during the 2002-2003 winter (Dec. 6, 7, and 12, 2002; Jan. 28, Feb. 3, and Mar. 11 and 12, 2003). We used the Max Planck Institut für Radio Astronomie 117-element bolometer array. The beams have a half-power width of 11″ and are separated by ∼20″. The instrument has a bandwidth of about 60 GHz, and an effective frequency close to 250 GHz (1.2 mm). Observations of 2002 TX_{300} were performed in "on-off" mode, in which the subreflector of the telescope was alternately (with a 2 Hz frequency) looking at the target and at a sky position 32″ away in azimuth (either to the left or right of the source, alternating every 10 s). While this procedure subtracts most of the atmospheric emission, the photometric accuracy is determined in part by the ability to eliminate its temporal fluctuations. Our multibeam observations allow us to estimate the latter from the channels adjacent to the central channel.

All bolometric measurements were obtained as "pooled observations" (i.e., service mode). Pointing and focus of the telescope were determined by measurements on the quasar 3C 454.3 and flux calibration on Uranus. The zenith atmospheric opacity at 250 GHz was measured from sky measurements at several elevations (skydip). Depending on the observing date, on-off measurements were performed during 15 to 40 min (4 to 10 loops of 20 10-s subscans, plus overheads). Observations were performed in good weather conditions (zenith sky opacity = 0.1–0.25). Atmospheric stability was good, except on Dec. 12 and Mar. 12 where large fluctuations of the opacity occurred. These two measurements were not considered, leaving us with a total of five individual measurements of 2002 TX_{300} 1.2 mm flux (see Table 2).

Data reduction was performed using both the NIC and MOPSI software packages, and very similar results were obtained. The basic reduction processes consist of I) despiking the data, II) computing the ON minus OFF phases III) reducing the sky noise by applying a noise removal algorithm based on beam-to-beam correlation IV) correcting the central channel flux by mean flux from adjacent channels, in order to remove possible residual continuum offsets.

3. Results and discussion

3.1. Variability

The time-resolved CCD photometry files were inspected for periodicities by means of the Lomb technique (Lomb 1976) as described in Press et al. (1992).

The periodogram of the Sierra Nevada data alone (see Fig. 1) shows a highly significant periodicity peak (exceeding the 99.9% confidence level) at 7.89 ± 0.03 h (3.04 ± 0.01 cycles per day). The periodogram shows other peaks located at approximately 4.04 cycles/day, 2.04 cycles/day, and 1.04 cycles/day. These peaks are daily aliases of the most significant

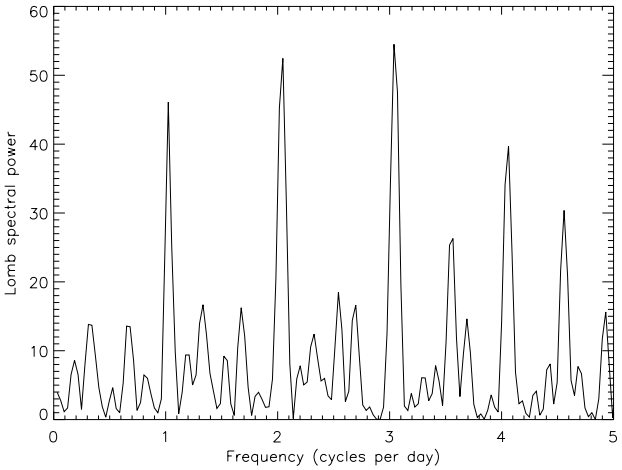

Fig. 1. Periodogram of the Sierra Nevada data. The highest peak corresponds to 3.04 cycles per day or approximately 7.89 h.

frequency. In particular, the peak at approximately 2.04 cycles/day or 11.8 h has a similar spectral power to the main peak, and therefore cannot be entirely ruled out as the actual rotation period. According to the periodogram, the most significant peak would imply a rotation period of either 7.89 h or 2 × 7.89 h depending on whether the lightcurve is single-peaked or double-peaked, respectively.

Using the few NOT data points one can also carry out a periodogram analysis. It turns out that the same high periodicity peak as in the Sierra Nevada data is also present in the NOT data, although the width of the peak is larger and the confidence level much lower, because of the few data points. From these data, the periodicity peak is at 7.8 ± 0.2 h.

The rotational phase curves which result from the combination of all the data sets using two different periods (the photometric one and twice that value) are shown in Fig. 2. In this figure, three kinds of lightcurves are shown. The raw data from the Sierra Nevada run are shown at the bottom, a median of those data in small phase bins is shown at the top, and the middle plot corresponds to the median of the Sierra Nevada data, as well as the NOT and CFHT data, all combined. Prior to combining all the data (normalized to their respective mean values), the observation times were corrected for light travel time. Comparing both figures, there is no clear indication that the lightcurve for the 7.89 h period is any better than for 2 × 7.89 h. Thus, we cannot conclude if the lightcurve is single-peaked or double-peaked, and therefore whether the actual spin period is 7.89 h or 15.78 h.

By fitting a sinusoidal function to the data, the amplitude of the lightcurve is 0.09 ± 0.08 mag. The fact that the amplitude of the 2002 TX_{300} lightcurve is small can indicate either that the variability is caused mainly by albedo distributions on the surface and/or by a slightly irregular shape. Another possibility is that the body is viewed nearly pole on. A double-peaked lightcurve could be an indication of irregularity, but as is well known, almost any lightcurve can be fitted by appropriate albedo distributions (Russell 1906) in a spherical body. Nonetheless, our lightcurve phased to a 2 × 7.89 h period does not show clear evidence of a double-peaked structure. If the

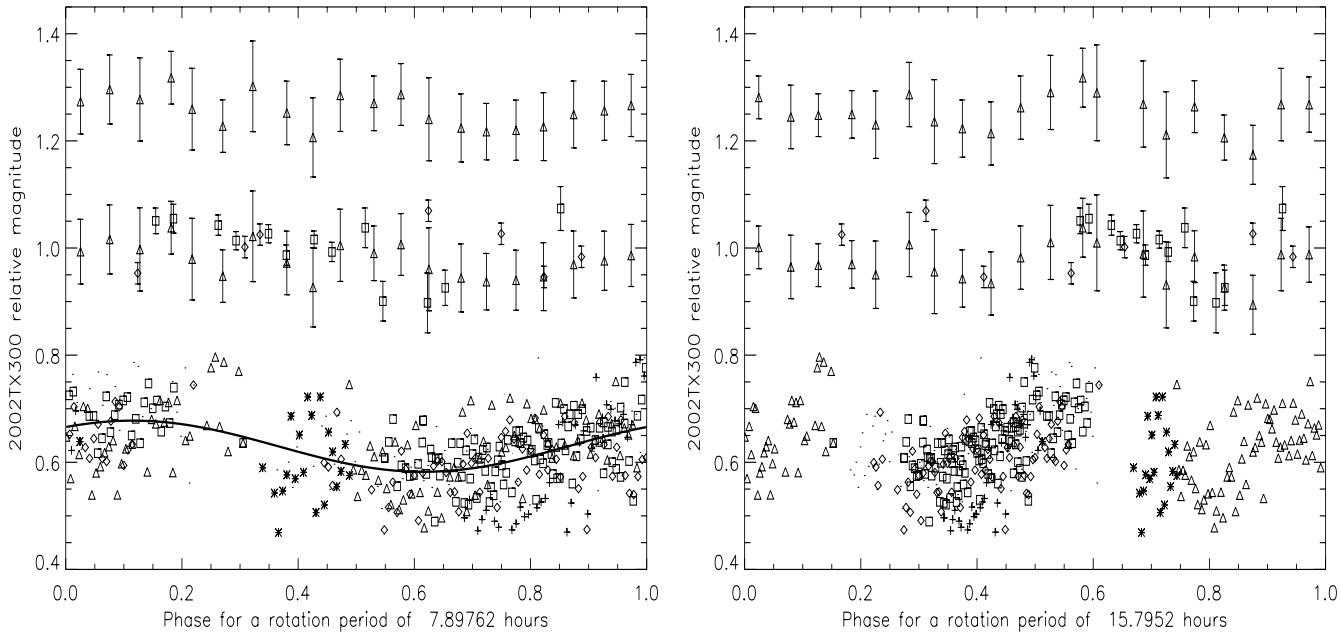

Fig. 2. *Left*: lightcurve of 2002 TX_{300} phased to a rotation period of 7.89762 h. The bottom plot corresponds to the raw Sierra Nevada data, with different symbols for the different dates of observation. A sinusoidal fit has been superimposed. The upper plot corresponds to the median of the Sierra Nevada data, in small phase bins. The middle plot shows the median of the Sierra Nevada data (triangles) as well as the NOT data (diamonds) and the CFHT data (squares). *Right*: same but for a rotation period of 15.7942 h.

observed variability were due to albedo variegations on the surface of a spherical body, the amplitude of the lightcurve would imply local albedo constrasts higher than 9%. On the other hand, if the variability were due to the elongation of the body, the amplitude would imply a minimum axial ratio of 1.09 for an aspect angle of 90 deg (1.25 if the aspect angle were 60 deg).

3.2. Lower limit for the density

By equating the spin period to the expression of the critical rotation period one can get a lower limit on the density. If the body is assumed to be spherical with no tensile strength, and rotating with a spin period of 7.89 h, the lower limit for the density to avoid spontaneous break up would be approximately 175 kg/m^3, using the expressions given in Davidsson (1999). If the spin period is 15.78 h, the lower limit to the density would then be approximately 43 kg/m^3. On the other hand, if the body is assumed to be prolate with no tensile strength, the lower limit for the density can be estimated from the expresions given by Davidsson (2001). For an axial ratio of 1.09 and assuming an aspect angle of 90 deg, the lower limits for the density would be 192 kg/m^3 if the body is rotating with a spin period of 7.89 h, or 48 kg/m^3 if the spin period is twice the photometric periodicity. The lower limit for the density would be larger for smaller aspect angles.

3.3. Average magnitudes and colors

In Fig. 3, the data in *BVRI* are shown. The average magnitudes for each band taken from the data shown in that figure are $B = 20.24 \pm 0.04$, $V = 19.59 \pm 0.06$, $R = 19.19 \pm 0.04$, and $I = 18.97 \pm 0.03$. Thus, the average $B-V$, $V-R$ and $R-I$ colors are 0.64 ± 0.07, 0.40 ± 0.07, and 0.22 ± 0.05, respectively.

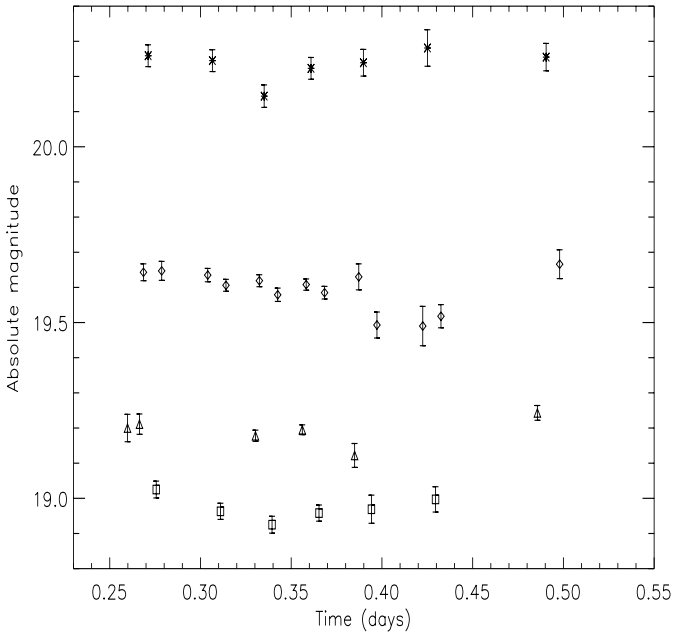

Fig. 3. *BVRI* magnitudes obtained from CFHT data. Asterisks represent the *B* data, diamonds correspond to *V*, triangles correspond to *R* data and squares correspond to *I* data.

3.4. Estimates of the albedo and size

The five individual measurements of 2002 TX_{300}'s 1.2 mm flux are summarized in Table 2. Averaging the five flux

measurements of Table 1 formally gives a mean flux of 0.22 ± 0.51 mJy. From this result we finally conclude that the object is not detected in our bolometric observations and adopt a 1-σ (resp. 2-σ and 3-σ) upper limit of 0.51 (resp. 1.02, 1.53) mJy for its 1.2 mm flux. The values pertain to mean helio- and geo-centric distances r_h = 40.764 AU and Δ = 40.969 AU, respectively. We can combine all the data sets to derive meaningful information on albedo and size. As previously discussed in the case of Varuna (Lellouch et al. 2002) for which the general equations were given, the thermal flux of a dark and quickly rotating TNO, assumed spherical, is primarily dependent on its diameter. The thermal flux also depends on the object emissivity and on orientation parameters (i.e. the sub-Earth and sub-solar latitudes), but is rather insensitive to the precise value of visible geometric albedo p_v and thermal inertia Γ. The relative independence on albedo stems from the $(1\text{-}A_b)^{0.25}$ dependence of the equilibrium temperature, where A_b, the Bond albedo, is likely to be even smaller than p_v, given the observed correlation of phase integral (q) with p_v for airless bodies (Lellouch et al. 2000a). A typical value of A_b = 0.03 can be adopted, corresponding e.g. to p_v = 0.08 and q = 0.4. The independence on thermal inertia is due to the fact that with a period of several hours and a typical temperature of ∼40–45 K, the thermal parameter Θ (defined e.g. in Spencer et al. 1989) is much larger than 1 for any plausible value of Γ, so that surface temperatures are independent on local time, i.e. constant over latitude bands ("fast rotator" regime). In contrast, the temperature vs. latitude function is strongly dependent on the sub-solar latitude, which is unknown given the unconstrained polar axis direction. In Varuna's case, the presence of a well-marked visible lightcurve argued in favor of a sub-solar (β_S) and sub-Earth (β_E) latitude close to 0° (Lellouch et al. 2000a). For 2002 TX_{300}, we consider two limiting cases: (i) $\beta_S \sim \beta_E \sim 0°$ (Sun and Earth in Equatorial plane) and (ii) $\beta_S \sim \beta_E \sim 90°$ (Sun and Earth on Polar axis, with one hemisphere entirely in shadow). The local temperature is also a function of the surface bolometric emissivity (ϵ_b), and the emitted thermal flux additionally depends on the spectral emissivity at the wavelength of the measurements (ϵ_λ). These parameters are entirely unknown for TNOs, and by analogy with Pluto (Lellouch et al. 2000a,b), we adopt ϵ_b = 0.9 and ϵ_λ = 0.7. We finally neglect any beaming effect for the thermal radiation. Maximum surface temperatures for the two cases are indicated in Table 3, as well as the 1-, 2- and 3-sigma upper limits on the object diameter.

Visible measurements, as described above, indicate a mean magnitude V = 19.605 on Oct. 30, 2002, i.e. at r_h = 40.741 AU, Δ = 39.902 AU. Neglecting any phase effects, the upper limits on the diameter, along with this value of V, imply lower limits to the object albedo, as detailed in Table 3. Adopting the 2-σ confidence level, and taking the mean values for the two orientation models discussed above, we conclude that 2002 TX_{300} has a maximum equivalent diameter of 907 km and a minimum visible geometric albedo of 8.4%. A tighter 3-σ confidence level implies a maximum diameter of 1110 km and a minimum V geometric albedo of 5.6%. Since the object has virtually the same color ($V - R$ = 0.40) as the Sun ($V - R$ = 0.36), this lower limit is also very close for the red albedo (8.7%, 5.3% for 2-σ and 3-σ respectively).

Table 2. IRAM 30-m observations.

Date	UT [a]	τ [b]	F [c] (mJy)
2002/12/06	20.0	0.20	0.7 ± 1.0
2002/12/07	18.6	0.10	0.8 ± 1.0
2003/01/28	20.8	0.10	0.3 ± 1.7
2003/02/03	16.0	0.20	−1.0 ± 1.3
2003/03/11	17.1	0.20	−0.2 ± 1.1

[a] UT time at the middle of integration.

[b] Mean zenith atmospheric opacity at 250 GHz.

[c] Flux from 2002 TX_{300}.

2002 TX_{300}'s visual geometric albedo is therefore larger than the canonical 0.04 value of cometary nuclei. Varuna's albedo has been measured by Jewitt & Sheppard (2002) and Lellouch et al. (2002). Quaoar's albedo has also been reported (Brown & Trujillo 2004), as well as the albedo of object 2003 AW_{197} (Margot et al. 2002).

Judging from the lower limit to the albedo of 2002 TX_{300} derived here and the values of the few other large TNOs whose albedos have been measured (see Table 4), it appears that TNOs might be intrinsically brighter than most comet nuclei, although this might be the case of just the largest TNOs, or of TNOs with high inclination orbits, like the brightest TNOs discovered so far. More light on this issue will be shed when the albedos of more, including fainter, TNOs will be measured by SIRTF, and later by Herschel.

4. Summary and conclusions

From a large set of observations of 2002 TX_{300}, short-term variability with a peak to peak amplitude of 0.09 ± 0.08 mag has been detected. The photometric period is 7.89 ± 0.03 h and the variability can be caused by albedo distributions on the surface, by irregular shape or by a combination of both effects. We do not have convincing arguments to favor any of the possibilities yet. In particular, we cannot determine whether the rotation period is 7.89 h or twice that value. By combining the data in the visible with the thermal observations at 1.2 mm, a lower limit of 0.056 to the V geometric albedo and an upper limit of 1110 km to the size of the object have been obtained at the 3-σ level. The object shows approximately neutral colors.

Acknowledgements. We are grateful to the Sierra Nevada Observatory staff. This research was partially based on data obtained at the Observatorio de Sierra Nevada which is operated by the Instituto de Astrofísica de Andalucía, CSIC. Part of the data presented here were taken using ALFOSC, which is owned by the Instituto de Astrofisica de Andalucia (IAA) and operated at the Nordic Optical Telescope under agreement between IAA and NBIfAFG of the Astronomical Observatory of Copenhagen. We thank the IRAM director for allocating Discretionary Time to this project. This work was supported by contracts PNE-001/2000-C-01, AYA-2001-1177, AYA2001-2089 and AYA-2002-0382. European FEDER funds for these contracts are also acknowledged.

Table 3. Temperature/Diameter/Albedo information.

Model	Max. temperature	Diameter (km)			p_v		
		1-σ	2-σ	3-σ	1-σ	2-σ	3-σ
$\beta_S = \beta_E = 0°$	47.2 K at Equator	<679	<961	<1177	>0.15	>0.075	>0.05
$\beta_S = \beta_E = 90°$	62.8 K at Pole	<602	<852	<1043	>0.19	>0.095	>0.063

Table 4. List of albedos of large TNOs.

Object	Geometric albedo p_v	Reference
Quaoar	0.12	(1)
Varuna	0.07, 0.038	(2, 3)
2002 AW_{197}	0.10	(4)
2002 TX_{300}	>0.08 (2-σ)	this paper
	>0.06 (3-σ)	

(1) Brown & Trujillo (2004).
(2) Jewitt & Sheppard. (2002).
(3) Lellouch et al. (2002).
(4) Margot et al. (2002).

References

Brown, M. E., & Trujillo, C. A. 2004, AJ, in press
Davidsson, B. J. R. 1999, Icarus, 142, 525
Davidsson, B. J. R. 2001, Icarus, 149, 375
Jewitt, D. C., & Sheppard, S. S. 2002, AJ, 123, 2110
Lellouch, E., Laureijs, R., Schmitt, B., et al. 2000a, Icarus, 147, 220
Lellouch, E., Paubert, G., Moreno, R., & Schmitt, B. 2000b, Icarus, 147, 580
Lellouch, E., Moreno, R., Ortiz, J. L., et al. 2002, A&A, 391, 1133
Lomb, N. R. 1976, Astroph. Space Sci., 39, 447
Margot, J. L., Trujillo, C., Brown, M. E., & Bertoldi, F. 2002, Amer. Astron. Soc., DPS Meet., 34, 17.03
Press, W. H., Teukolsky, S. A., Vetterling, W. T., & Flannery B. P. 1992, in Numerical Recipes in Fortran: the art of scientific computing, 2nd edition (London: Cambridge Univ. Press), 569
Russell, H. 1906, ApJ, 24, 1
Sheppard, S., & Jewitt, D. C. 2002, AJ, 124, 1757
Spencer, J. R., Lebofsky, A. L., & Sykes, M. V. 1989, Icarus, 78, 337